Study of γ-Valerolactone as a Diesel Blend: Engine Performance and Emission Characteristics

Á. Bereczky[1*], K. Lukács[1], M. Farkas[2], S. Dóbé[2,*]

[1]Department of Energy Engineering, BME, Budapest, Hungary
[2]Institute of Materials and Environmental Chemistry, MTA TTK, Budapest, Hungary

Abstract
γ-valerolactone (GVL) is a C5-cyclic ester that can be produced from biomass providing a potentially renewable fuel for transportation and feedstock for the chemical industry. Experiments were performed with fossil diesel (D), D + biodiesel (BD) and D + BD + GVL blends. A four cylinder, turbocharged direct injection diesel engine was used for the tests. The engine was coupled to a dynamometer to vary the load. CO, NO_x, THC and smoke emissions were measured by using a multi-channel gas analyser. Compared with D, and D + BD blends, addition of GVL had relatively little effect on engine performance and NO_x emissions, but reduced the concentration of CO and smoke significantly.

Introduction

Energy security and concerns related to climate change as well as the need to provide subsistence for rural communities have lead to worldwide interest in the production of biofuels over the past decades. The principal biofuels under consideration are alcohols (most notably bioethanol) and methyl esters of long chain fatty acids (FAMEs), usually also referred to as "biodiesel", which are typically used blended in gasoline and fossil diesel, respectively.

Life-cycle analyses have questioned the sustainability of many first generation biofuels, such as corn ethanol, stimulating worldwide interest in second generation (2G) biofuels. 2G biofuels are produced from non-edible lignocellulosic raw materials, which constitute a huge renewable source of biomass providing the potential of mitigating global warming. In recent years, very efficient catalytic methods have been developed for the production of γ-valerolactone (GVL) from carbohydrates [1, 2] and even directly from biomass feedstock [3]. GVL is a valuable platform molecule for the production of fine chemicals and it has been widely considered as a potential biofuel for use in transportation. In fact, however, no detailed engine study with GVL or GVL fuel blends have been performed so far.

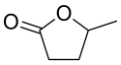

γ-valerolactone (GVL)

As part of an ongoing research program on the applicability of GVL as a fuel in IC engines, and concerning its combustion kinetics, and atmospheric chemistry, we report here our very first results. The effect of GVL on diesel engine performance, combustion characteristics and exhaust emissions was studied for assessing its potential as a diesel blend. Comparative experiments were performed with fossil diesel, biodiesel–diesel, and diesel–biodiesel–GVL fuels.

Our preliminary tests showed GVL to have a low cetane number (CN) and it is known to have a comparable low heating value (Table 1). These drawbacks may be compensated, however, by its potentially advantageous effects on the emission characteristics when used blended in fossil diesel. In particular, the reduction of smoke emission would be of great value. Particulates (PM) associated with diesel exhaust are of very small size, they have large surface areas with adsorbed species some of which are strongly mutagenic and carcinogenic [4]. Moreover, according to a very recent comprehensive study [5], the contribution of soot (black carbon) to global warming is much higher than previously thought. Its impact on the climate is larger than that of methane and roughly amounts to two-thirds of that of carbon dioxide. Note that diesel emissions are major sources of black carbon worldwide [4].

2. Experimental

2.1 Test Engine Setup

The test engine facility has been described previously [6-8]. It can be divided into three main parts: (*i*), the compression ignition engine coupled to a dynamometer, (*ii*), an exhaust gas analyzer and (*iii*), measurement control and data acquisition units.

An off-road, four-cylinder, turbocharged, direct injection, water-cooled diesel engine with exhaust gas recirculation (Audi-VW) was used to perform the experiments. The main technical specifications of the engine were the following: bore × stroke, 79.5 × 95.5 mm; compression ratio, 19.5:1; maximum power, 66 kW at 4000 rpm; peak torque, 202 Nm at 4000 rpm; injection pressure, 180 bar. The diesel fuels were introduced into the engine from a fuel tank equipped with a fuel mass flow meter (AVL 7030). All tests were performed on the unmodified diesel engine.

A Borghi & Saveri (type FE-350S) eddy-current dynamometer was used for loading the diesel

* Corresponding author: bereczky@energia.bme.hu
* Corresponding author: dobe.sandor@ttk.mta.hu

engine. It allowed the breaking load (*M*) and rotation speed (*N*) to be varied in a wide range independently from each other (maximum power 257 kW, maximum speed 8000 rpm, maximum torque 1400 N m).

A Horiba Mexa-820 exhaust gas analyzer was applied to analyze engine emissions. The Horiba system has different modules to measure a variety of chemical species including the regulated emissions of NO/NOx ($NO + NO_2$) using a chemiluminescence analyzer (H.CLD, CLA-53M), total unburned hydrocarbons (*THC*) using a flame ionization detector (H.FID, FIA-22), and CO/CO_2 using a nondispersive infrared (NDIR, AIA-23) detector. Before starting the measurements, the gas analyzer was calibrated by known gas mixtures. The emitted PM concentration was measured by a smoke meter (AVL-415). The sampling system was placed before the oxidation catalytic converter in the exhaust pipe of the engine. A K-type thermocouple (Omega Eng. Inc.) was used to monitor the exhaust gas temperature (EGT).

An integrated hardware-software system of units organised by a master PC and LabView programme made possible the on-line control of most of the experimental parameters and simultaneous measurement of engine performance and emission characteristics. The dynamometer settings and the engine throttle were controlled and the respective data acquired by a test assistant control system. Indication diagrams were obtained by measuring the pressure (*P*) inside one of the piston cylinders with a pressure transducer (Kistler KIAG 6031) which was connected to a charge amplifier. The crank angle (CA) positions needed were attained at the crankshaft by using an optical encoder (Hengstler RI32). The *P-CA* signals were fed into a SMETEC-COMBI PC indication system for data acquisition. The data acquisition system was externally triggered 1024-times in one revolution by the encoder. The measured emission, temperature and flow data were recorded also by a computer in real time.

2.2 Test Fuels

The fossil diesel (2-D), used as the base fuel and the biodiesel (FAME) were obtained from commercial sources in Hungary. GVL (≥98%, FCC, FG) was supplied by Sigma-Aldrich (SAFC). Some properties of these fuels are given in Table 1.

Solubility tests were made prior to the preparation of fuel blends by visual inspection. γ-valerolactone (GVL) was well miscible with biodiesel (BD), but showed poor solubility in conventional diesel fuel (<2.5v/v% at room temperature). In a three-component blend, biodiesel served as a co-solvent mitigating this effect to quite some extent. A mixture of 10:3:1 (v/v) = 71.4% diesel (D) : 21.5% biodiesel (BD) : 7.1% γ-valerolactone (GVL) was found stable for a prolonged time at room temperature.

Table 1
Selected properties of fuels used in the experiments

Property	**Diesel (2-D)**	**Biodiesel (FAME)**	**GVL**
Lower heating value (MJ/kg)	43	~39	27
Density (g/cm^3), 15 °C	0.82	0.86–0.90[a]	1.04
Kinematic viscosity (mm^2/s), 40 °C	2.5	3.5–5.0[a] 1.9–6.0[b]	2.1
Flash point (°C)	66	>120[a] >130[b]	96
Composition (wt%)			
C	87	77	60
H	13	12	8
O	0	11	32
Cetane number	55	>51[a] >47[b]	<10[c]

[a] EN 14214 limit. [b] ASTM D675 limit. [c] Determined by the standard test method EN ISO 5165:1999.

3. Results and Discussion

3.1 Operating Conditions

Engine performance and emission tests were carried out by using the following fuels: (*i*), 100% D; (*ii*), 76.9% D + 21.5% BD and, (*iii*), 21.4% D + 21.5% BD + 7.1% GVL. The varied experimental parameters were the engine break torque (*M*), i.e., load, and the engine speed (*N*). The break torque was set, on average, to 44, 87, 131 and 172 N m corresponding to 25, 50, 75 and 100% engine load, respectively. Tests were made at the engine rotational speeds of 1900, 2000, 2200, 2500 and 3000 rpm. Experiments with the different fuel blends were conducted back-to-back by maintaining the very same operational conditions in each run; measurements were done at 11 work points.

Several performance parameters and emission data were determined among which we report and discuss here the break power (*BP*), break specific fuel consumption (*BSFC*), break thermal efficiency (*BTE*) and *P-CA* indicator diagrams, as well as the exhaust gas concentrations for total unburned hydrocarbons (*THC*), carbon monoxide (CO), nitrogen oxides (NO_x) and smoke (*PM*).

3.2 Engine Performance

Break Power. Fig.1 shows the variation in engine power at maximum load with different engine speeds. As seen, there are no noticeable differences in the measured power output between the studied 100% D and 77% D + 23% BD fuels. Inclusion of GVL, that is, the use of the blend 71% D + 22% BD + 7% GVL results in systematically, but only slightly lower *BP*: on average, the engine power is less by 3.2% compared with the neat diesel fuel case. The reduction of break power by GVL is in accordance with the significantly lower calorific value of this blend component (Table 1). Biodiesel has also lower heating value than fossil diesel, but the reduction in break power for the D-BD blend is somewhat less than expected because of the possible

power recovery effects [9-11]. The brake power increases with the increase of engine speed approximately linearly up to ~2500 rpm for all tested fuels. At even higher speed, the change becomes slower likely due to a growing increase of engine friction losses.

BP has been found to increase linearly at constant speed with the increase of engine load which is the expected behaviour and reflects essentially the consistency of the results obtained with the current test apparatus.

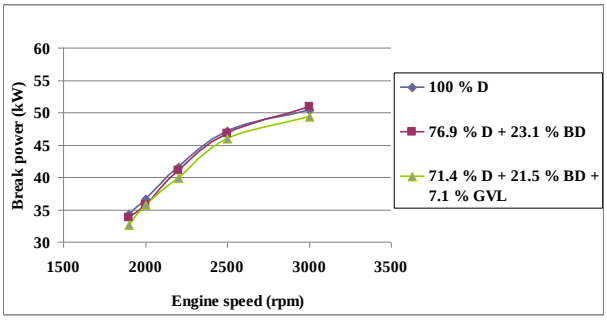

Fig.1. *BP* at full load as a function of engine speed for D, D–BD and D–BD–GVL blends.

Break Specific Fuel Consumption. Variation of *BSFC* with engine speed at maximum load is presented in Fig.2. The best performance was provided by the neat diesel fuel, while the three-component blend showed the highest specific fuel consumption. On average, *BSFC* for the (77% D + 23% BD) was higher by 2.7%, and that for the (71% D + 22% BD + 7% GVL) blend higher by 6.8% compared with 100% D.

BSFC is seen to go through a minimum at around 2400-2500 rpm with increasing engine speed (Fig.2). Similar *BSFC* curve was reported in the literature, e.g. in [12] and [13]. One possible explanation of the observed trend is that at lower speeds *BSFC* increases due to increased time for heat losses from the gas to the cylinder and piston wall and because of low the charging pressure, while at high rotational speeds, the increasing frictional losses reduce the fuel efficiency [14].

With the decrease in load, the *BSFC* decreases (Fig.3), but the trend remains the same for the three fuels as noted above. This observation may be explained by the higher percentage of increase in break power with load as compared to fuel consumption [9].

It is generally accepted that the fuel consumption of a diesel engine operated with biodiesel or oxygenate blends is higher compared to the base-line fossil diesel because of the need to compensate for the loss of heating values of the blending fuel components (see, e.g., in [7] and the recent review paper by Xue et al. [9]). Basically, this effect explains the higher specific fuel consumption for the diesel-biodiesel and diesel-biodiesel-GVL blends we have observed in our current work. The heating values of the 77% D + 23% BD and 71% D + 22% BD + 7% GVL blends are lower by ~2.3% and ~4.7%, respectively, compared to fossil diesel. These figures are to be compared with the respective increase in fuel consumption by 2.7% and 6.8%. Beside the lower heat content, the higher density and higher viscosity of BD and GVL, as well as the engine type and operating conditions also affect the fuel efficiency that may serve as an explanation for the slightly higher fuel consumption than expected by the differences in the heating values.

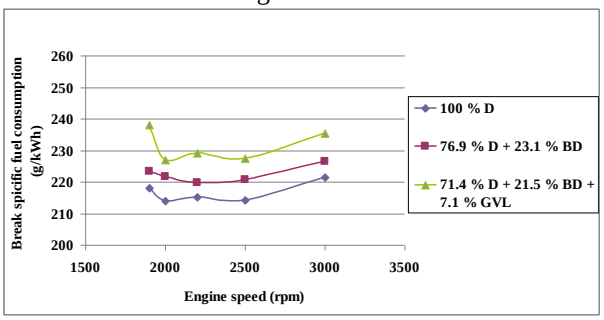

Fig.2. *BSFC* at full load as a function of engine speed.

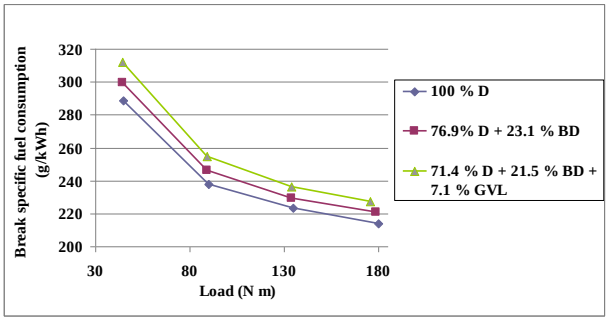

Fig.3. Variation of *BSFC* at 2500 rpm engine speed with 25, 50, 75 and 100% loads.

Break Thermal Efficiency. Fig.4 shows the variation of *BTE* vs. engine speed at maximum load and Fig.5 gives its variation on engine load at 2500 rpm. The *BTE–N* curves first increase, then decrease with increasing rotational speed, the maxima being at around 2500 rpm (Fig.4). The observed maximal thermal efficiency is practically the same for the three fuels studied: 38.8 ± 0.1%. *BTE* is the reciprocal of *BSFC* normalized to the heating value of the fuel. Thus, the observations concerning *BTE* are fully consistent with the slight increase of the fuel consumption for the D-BD and D-BD-GVL blends due to their lower heating values as discussed in the previous paragraph.

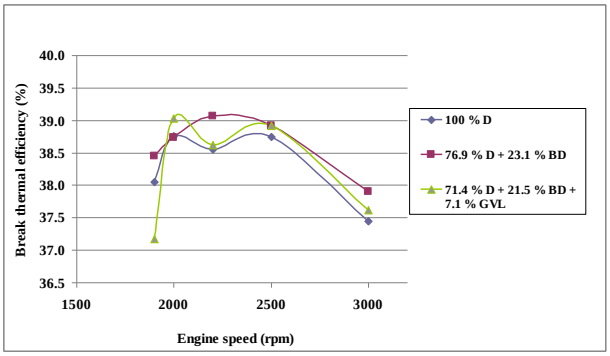

Fig.4. *BTE* at full load as a function of engine speed.

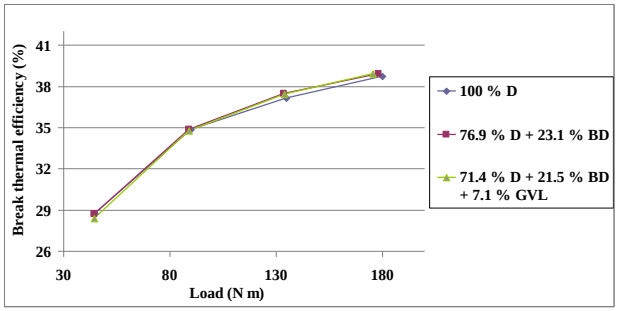

Fig.5. Variation of *BTE* at 2500 rpm engine speed with 25, 50, 75 and 100% loads.

Indicator Diagram. Fig.6 displays a representative example (50% load at 2500 rpm) of the measured in-cylinder pressure (*P*) versus crank angle (*CA*) data for the three fuels under study. The *P–CA* traces shown present a typical bimodal pressure history characteristic for CI engines indicating a phase of premixed combustion followed by a phase of diffusion combustion [14]. The *P-CA* diagrams revealed little change with change of fuels under all conditions similar to the 50% load and 2500 rpm case depicted in Fig.6. Consequently, the rate of heat release was also very similar for the D, D-BD and D-BD-GVL fuel samples under the same operating conditions [15]. These features which are attributed to the underlying combustion processes in the engine are consistent with the observed relatively small variation of the performance parameters of the tested three fuels.

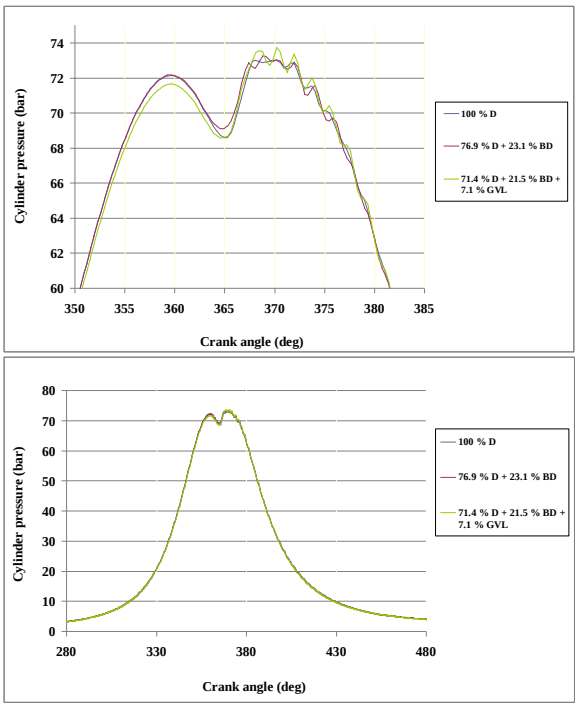

Fig.6. In-cylinder pressure (*P*) versus crank angle (*CA*) at 50% load and 2500 rpm engine speed.

3.2 Exhaust Emissions

Total Unburned Hydrocarbons (THC). At maximum load of the engine, the unburned HC in the exhaust gas was significantly less when the fossil diesel was replaced by the diesel-biodiesel blend, and it was even further reduced in the case of the GVL-containing fuel (Fig.7). However, in practical applications when the engine is operated at lower loads, this advantageous effect would be less pronounced (Fig.8). One straightforward explanation for the reduced *THC* is the oxygen content of BD and GVL which may lead to more complete combustion [9, 16, 17].

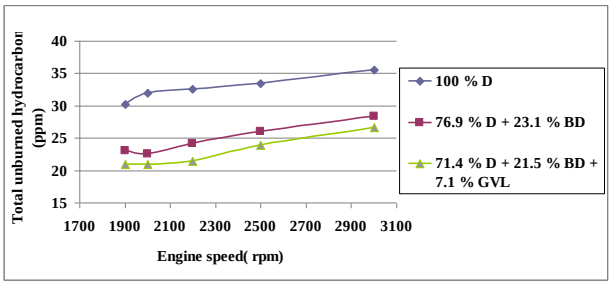

Fig.7. Emitted *THC* at full load as a function of engine speed.

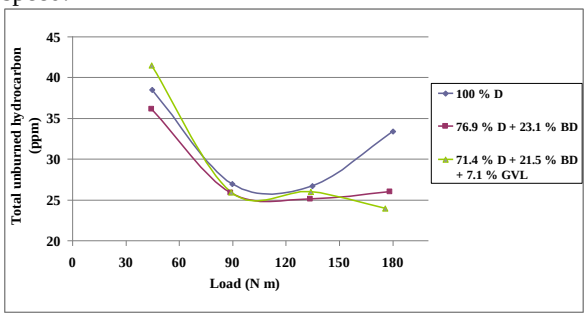

Fig.8. Variation of *THC* at 2500 rpm engine speed with 25, 50, 75 and 100% loads.

Carbon monoxide (CO). The emitted CO at full engine load was reduced very significantly by the oxygen-containing blending components in the medium range of engine speed (Fig.9). On the other hand, the CO concentration was practically the same for all three fuels tested and increased with decreasing engine load at constant rotational speed (Fig.10). This latter observation can be explained by that lower loads result in lower combustion temperature giving rise to less complete combustion and hence an increased emission of CO [7, 18]. Most of the papers in the literature report that CO emissions reduce when fossil diesel is replaced by biodiesel or biodiesel-oxygenate blends due to the higher oxygen content and lower carbon to hydrogen ratio [9] of these fuels which is basically consistent with our present findings.

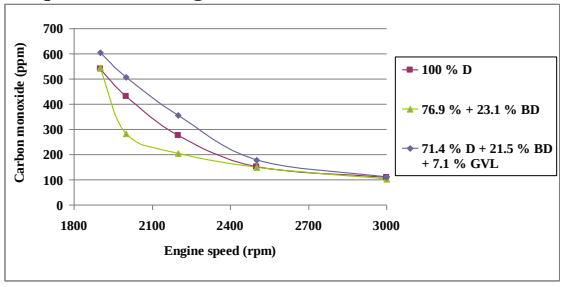

Fig.9. Emitted CO at full load as a function of engine speed.

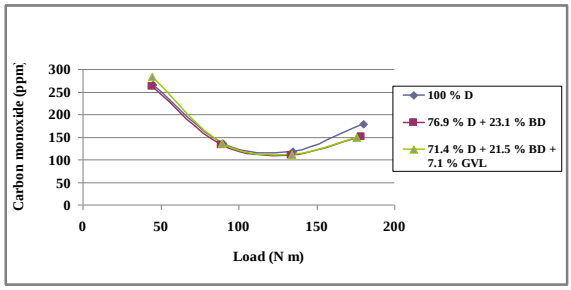

Fig.10. Variation of CO at 2500 rpm engine speed with 25, 50, 75 and 100% loads.

Nitrogen Oxides (NO_x). NO_x formation was found to decrease with an increase in engine speed at full load (Fig.11) that may have been primarily caused by a shorter residence time that was available for NO_x formation [9, 11]. As load grew (Fig.12), the temperature became higher in the combustion chamber and NO_x increased due to the strong temperature dependence of its formation [19, 20]. Favourably, the NOx emissions were very close to each other concerning the tested three fuels in contrast with many literature sources that reported an increase of NO_x when blends of biodiesel or other oxygenates were compared with conventional diesel fuel [9, 19].

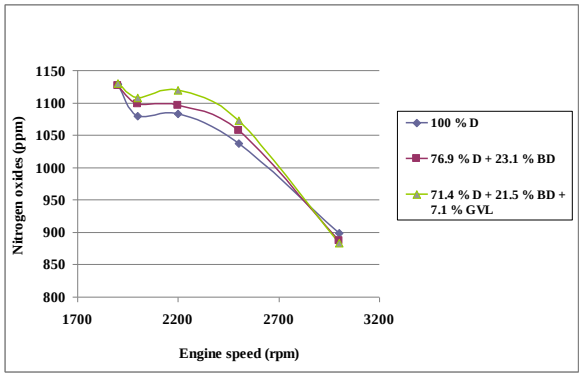

Fig.11. Emitted NO_x at full load as a function of engine speed.

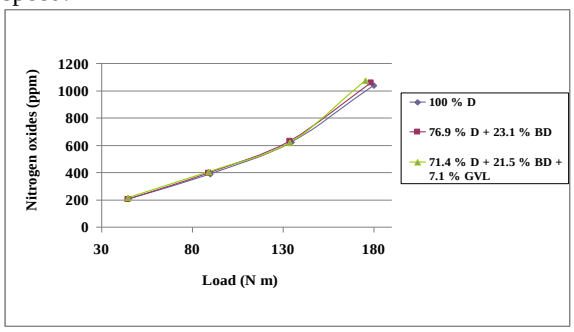

Fig.12. Variation of NO_x emission at 2500 rpm engine speed with 25, 50, 75 and 100% loads.

Smoke (PM). The emitted smoke concentrations are shown in Fig.13 and Fig.14 as a function of engine speed at 100% load and plotted against the engine load at 2500 rpm, respectively. A very significant decrease in *PM* was observed when fossil diesel was replaced by the tested blends. At full load, the average reduction in smoke was 23% for the 77% D + 23% BD blend, and it was 47% for 71%D + 22% BD + 7% GVL compared to 100% D. The reducing effect was more pronounced at high engine loads and slower rotations, but it was significant at all conditions. Also, the trend remained the same, including the effect of GVL to provide an additional reduction of smoke emissions.

The *PM* concentration in the exhaust decreased with increasing engine speed for the tested three fuels (Fig.13). Similar observation was reported in several other papers in the literature and attributed to an increase in turbulence effects which enhance the extent of complete combustion [9]. At constant speed the increased engine load was found to result in higher *PM* emission (Fig.14) which can be understood by the effect of increased fuel amount, decreased air-to-fuel ratio and hence a less complete combustion (see, e.g. [21] and the review by Xue et al. [9]).

Our results support the conclusion of most of the literature studies that biodiesel and other oxygenates reduce the smoke emission of diesel engines by providing extra oxygen for a more complete combustion [9]. In several works, e.g. in [22] and as presented in the thorough literature overview by Boot and co-workers [23], a strong reduction of smoke with the increase of oxygen mass fraction of diesel blends was reported. We have experienced similarly strong decrease by using GVL as a blending agent. GVL has high oxygen content (Table 1) and, although it was used just in 7%, it had increased the oxygen mass fraction in the three-component diesel blend substantially giving rise to a drop in the *PM* concentrations compared to both the D and D + BD fuel samples. Beside the oxygen mass fraction, the molecular structure of the oxygenate plays also a role in the sooting behaviour. Boot and co-workers observed a extraordinary large smoke reduction by blending cyclohexanone to fossil diesel [23]. Cyclohexanone, similarly to GVL, is a cyclic oxygenate, it also has low cetane number (low reactivity) and relatively low heating value. The strong reduction of particulate emissions by cyclic oxygenates can be due to their enhanced trapping efficiency in converting fuel carbon into non-sooting species hindering the formation of the first ring structures of soot formation.

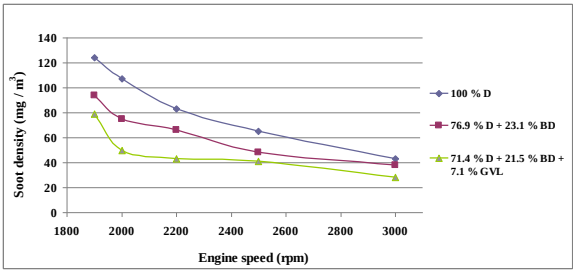

Fig.13. Emitted smoke concentration at full load as a function of engine speed.

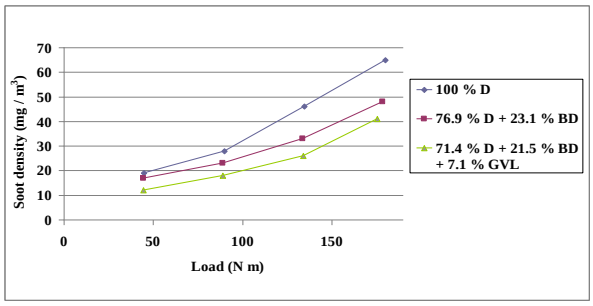

Fig.14. Variation of smoke emission at 2500 rpm engine speed with 25, 50, 75 and 100% loads.

4. Conclusions

(*i*) The best engine performance, concerning power and fuel consumption was observed with 100% fossil diesel (D), but it was practically the same with the 77% D + 23% biodiesel (BD) blend and was worse only slightly when the 71% D + 22% BD + 7% GVL blend was used in the experiments.

(*ii*) The *THC* and CO emissions decreased substantially in the order of the fuels D > D + BD > D + BD + GVL. Favourably, and in contrast with many literature reports, we did not observe noticeable enhancement of NO_x emissions by using the oxygenated blending components BD and GVL.

(*iii*) The smoke concentration of the exhaust was diminished significantly with the D + BD fuel compared to neat diesel, and it was even further reduced, on average by 47% using the GVL-containing blend.

Acknowledgements

This work has been supported by the Hungarian Research Fund OTKA (contract OMFB-00992/2009). This work is connected also to the scientific program of "Development of quality-oriented and harmonized R+D+I strategy and functional model at BME" (ID: TÁMOP-4.2.1/B-09/1/KMR-2010-0002) project The authors appreciate the technical assistance in the experiments by Drs I. Szilágyi and G. L. Zügner as well as the undergraduate students Messrs Á. Baksza, Á. Illés, D. Kiss, A. Pap and D. Szép.

References

1. I. Horváth; H. Mehdi; V. Fábos; L. Boda; L. Mika, Green Chemistry (2008) 238-242
2. H. Mehdi; V. Fábos; R. Tuba; A. Bodor; L. Mika; I. Horváth, Topics in Catalysis (2008) 49-54.
3. A. Galletti; C. Antonetti; E. Ribechini; M. Colombini; N. Di Nasso; E. Bonari, Applied Energy 102 (2013) 157-162.
4. J. Gaffney; N. Marley, Atmospheric Environment 43 (1) (2009) 23-36.
5. J. Tollefson, Nature News (2013) doi: 10.1038/nature.2013.12225.
6. F. Lujaji; A. Bereczky; M. Mbarawa, Energy & Fuels 24 (2010) 4490-4496.
7. F. Lujaji; L. Kristóf; A. Bereczky; M. Mbarawa, Fuel 90 (2) (2011) 505-510.
8. T. Kivevele; L. Kristóf; A. Bereczky; M. Mbarawa, Fuel 90 (8) (2011) 2782-2789.
9. J. Xue; T. Grift; A. Hansen, Renewable & Sustainable Energy Reviews 15 (2) (2011) 1098-1116.
10. S. Basha; K. Gopal; S. Jebaraj, Renewable & Sustainable Energy Reviews 13 (6-7) (2009) 1628-1634.
11. E. Buyukkaya, Fuel 89 (10) (2010) 3099-3105.
12. H. Hazar, Renewable Energy 34 (6) (2009) 1533-1537.
13. A. Pal; A. Verma; S. Kachhwaha; S. Maji, Renewable Energy 35 (3) (2010) 619-624.
14. J. B. Heywood, Internal Combustion Engine Fundamentals, McGraw-Hill, Inc., New York, St Louis, etc, 1988.
15. Á. Bereczky; K. Lukács; M. Farkas; S. Dóbé: to be published, 2013.
16. A. Tsolakis; A. Megaritis; M. Wyszynski; K. Theinnoi, Energy 32 (11) (2007) 2072-2080.
17. F. Wu; J. Wang; W. Chen; S. Shuai, Atmospheric Environment 43 (7) (2009) 1481-1485.
18. H. Chen; J. Wang; S. Shuai; W. Chen, Fuel 87 (15-16) (2008) 3462-3468.
19. K. Varatharajan; M. Cheralathan, Renewable & Sustainable Energy Reviews 16 (6) (2012) 3702-3710.
20. J. Warnatz; U. Maas; R. W. Dibble, Combustion: Physical and Chemical Fundamentals, Modelling and Simulation, Experiments, Pollutant Formation, Springer-Verlag, Heidelberg, New-York, 2001.
21. H. Raheman; S. Ghadge, Fuel 86 (16) (2007) 2568-2573.
22. Y. Ren; Z. Huang; H. Miao; Y. Di; D. Jiang; K. Zeng; B. Liu; X. Wang, Fuel 87 (12) (2008) 2691-2697.
23. M. Boot; P. Frijters; C. Luijten; B. Somers; R. Baert; A. Donkerbroek; R. Klein-Douwel; N. Dam, Energy & Fuels 23 (2009) 1808-1817.